

# Comparison of the Direct Numerical Simulation of Zero and Low Adverse Pressure Gradient Turbulent Boundary Layers

V. Kitsios, C. Atkinson, J.A. Sillero, G. Borrell, A. Gul Gungor, J. Jiménez and J. Soria

**Abstract** Statistics from the direct numerical simulation (DNS) of an adverse pressure gradient (APG) turbulent boundary layer (TBL) are presented. Flow simulations are performed using a TBL DNS code with the desired APG applied via a tailored farfield boundary condition. The APG TBL has a maximum momentum thickness based Reynolds number ( $Re_{\delta_2}$ ) of 6000, and a near constant ratio of pressure velocity to freestream velocity, over a range of  $Re_{\delta_2}$  from 3000 to 5000. Streamwise velocity variance profiles are shown to collapse under outer velocity scaling as opposed to friction velocity scaling over this range.

## 1 Introduction

The separation of turbulent boundary layers (TBL) arise from the application of adverse pressure gradients (APG). Engineering systems operating in such environments include aircraft wings, wind turbine blades, and turbo-machinery. Flow separation in these systems has a significant impact on performance/efficiency, and in some cases may lead to catastrophic consequences. The accurate prediction of TBL separation remains a significant challenge for engineering design. An additional complexity of these aerofoil geometries is that the pressure gradient is constantly

---

V. Kitsios (✉) · C. Atkinson

Laboratory for Turbulence Research in Aerospace and Combustion,  
Department of Mechanical and Aerospace Engineering, Monash University,  
Melbourne, Australia  
e-mail: vassili.Kitsios@monash.edu

J.A. Sillero · G. Borrell · J. Jiménez  
School of Aeronautics, Universidad Politécnica de Madrid, Madrid, Spain

A.G. Gungor  
Department of Astronautical Engineering, Istanbul Technical University, Istanbul, Turkey

J. Soria  
Department of Aeronautical Engineering, King Abdulaziz University,  
Jeddah, Kingdom of Saudi Arabia

© Springer-Verlag Berlin Heidelberg 2016  
Y. Zhou et al. (eds.), *Fluid-Structure-Sound Interactions and Control*,  
Lecture Notes in Mechanical Engineering,  
DOI 10.1007/978-3-662-48868-3\_26

changing in the streamwise direction, as in the large eddy simulation of Kitsios et al. (2011).

In order to decouple the effect of the surface curvature from the influence of the local pressure gradient, it is instructive to consider the case of a canonical self-similar APG TBL on a flat surface. A self-similar APG TBL is one in which each of the terms in the Navier-Stokes equations have the same proportionality with streamwise position. The DNS of relatively low Reynolds number self-similar APG TBLs have previously been studied in Lee and Sung (2008). A higher Reynolds number separated non-self-similar APG TBL was simulated and studied in Gungor et al. (2012). In the present study we undertake a DNS of a self-similar APG TBL of maximum momentum thickness based Reynolds number  $Re_{\delta_2} \equiv U_e \delta_2 / \nu = 6000$ , where  $\delta_2$  is the momentum thickness,  $\nu$  is the kinematic viscosity, and  $U_e$  is the velocity at the edge of the boundary layer of height  $\delta$ . We are particularly interested in the incipient separation case in which the skin friction approaches zero.

## 2 Direct Numerical Simulation Solver

We adopt the hybrid MPI and openMP parallelised DNS code of Simens et al. (2009) and Borrell et al. (2013), with the farfield boundary condition (BC) modified to achieve the desired APG flow. The code solves the Navier-Stokes equations of constant density ( $\rho$ ) and constant  $\nu$ , in a three-dimensional rectangular volume. The flow directions are the streamwise ( $x$ ), wall-normal ( $y$ ) and spanwise ( $z$ ), with associated velocity components  $U$ ,  $V$  and  $W$ . A Fourier decomposition is used to represent the flow in the periodic spanwise direction, with the compact finite difference method of Lele (1992) used in the aperiodic streamwise and wall-normal directions. The modified three sub-step Runge-Kutta scheme of Simens et al. (2009) is used to step the equations forward in time.

The boundary conditions of the original ZPG version of the TBL DNS code are as follows. The bottom surface is a flat plate with a no-slip (zero velocity) BC. The spanwise boundaries are periodic. Following Sillero et al. (2013) the flow at the inlet is a zero pressure gradient (ZPG) TBL specified by mapping and rescaling a streamwise wall-normal plane from a downstream station, which in the present simulations is at position  $x_r = 60\delta(x_0)$ , where  $\delta(x_0)$  is the boundary layer thickness at the inlet. At the farfield boundary the spanwise vorticity is zero, and the wall normal velocity is

$$V_{ZPG}(x) = \frac{d\delta_1}{dx} U_{ZPG}, \quad (1)$$

where  $\delta_1$  is the displacement thickness, and  $U_{ZPG}$  is the constant freestream streamwise velocity of the ZPG TBL (Sillero 2014).

In order to generate the desired self-similar APG TBL flow the farfield wall normal velocity BC must be modified. In the APG TBL DNS, to allow the rescaling necessary for the inlet boundary condition an initial ZPG TBL is simulated up until the streamwise position  $x_s = 100\delta(x_0)$  (located after the recycling plane) by applying  $V_{ZPG}(x)$  at the farfield boundary as defined in (1). Note  $\delta(x_0)$  is the boundary layer thickness at the inlet. Downstream of the position  $x_f = 140\delta(x_0)$  the APG farfield wall normal velocity,  $V_{APG}(x)$ , is applied. The wall normal component,  $V_{APG}(x)$ , is related to the streamwise freestream velocity,  $U_{APG}(x)$ , via the boundary layer streamfunction solution in the farfield, where  $U_{APG}(x) \propto x^{-0.23}$  for the desired incipient separation case (Mellor and Gibson 1966). From  $x_s$  to  $x_f$  the APG BC is introduced in the streamwise direction via a smoothing function.

The domain extents in the streamwise, wall normal and spanwise directions are  $(L_x, L_y, L_z)/\delta(x_0) = (801, 38, 134)$  for the ZPG TBL DNS and  $(L_x, L_y, L_z)/\delta(x_0) = (801, 70, 134)$  for the APG case. The associated number of grid points are  $N_x \times N_y \times N_z = 8193 \times 315 \times 1362$  for the ZPG and  $N_x \times N_y \times N_z = 8193 \times 500 \times 1362$  for the APG. The APG simulation has a larger wall normal domain ( $L_y$ ) and more points in this direction ( $N_y$ ) due to the APG TBL expanding more quickly in the streamwise direction than the ZPG TBL. Both simulations have the same grid spacings of  $(\Delta x, \Delta y_{wall}, \Delta y_{\infty}, \Delta z)/\delta(x_0) = (0.1, 0.003, 0.17, 0.1)$ , where  $\Delta x$  and  $\Delta z$  are the constant spacing in the streamwise and spanwise directions, with  $\Delta y_{wall}$  and  $\Delta y_{\infty}$  the wall normal grid spacing at the wall and at the farfield boundary respectively. The cell spacings in viscous units are given by  $(\Delta x^+, \Delta y_{wall}^+, \Delta y_{\infty}^+, \Delta z^+) \equiv (\Delta x, \Delta y_{wall}, \Delta y_{\infty}, \Delta z)u_{\tau}/\nu$ , where friction velocity  $u_{\tau} = \sqrt{\tau_w/\rho}$ , with  $\tau_w$  the mean shear stress at the wall. Using the friction velocity at the inlet as a worst case scenario  $(\Delta x^+, \Delta y_{wall}^+, \Delta y_{\infty}^+, \Delta z^+) = (14, 0.41, 25, 14)$ . In both simulations the Courant number was set to unity, with an average time step size of approximately  $0.05U_e(x_0)/\delta(x_0)$ . Statistics were accumulated over 22,000 time steps or equivalently 642 eddy-turnover times, where one eddy-turnover time is defined as  $\delta(x_0)/u_{\tau}(x_0)$ .

### 3 Results

The ZPG and APG boundary layers are first compared on the basis of  $Re_{\delta_2}$ , and the friction and pressure velocity scales. The streamwise velocity variance profiles from various streamwise positions are then non-dimensionalised on the basis of  $u_{\tau}$  and  $U_e$  to determine the most appropriate scaling. In all of the following figures the green and red lines represent the ZPG and APG cases respectively.

The momentum thickness based Reynolds number illustrated in Fig. 1a, clearly increases in the APG TBL more rapidly than the ZPG TBL, due to the former expanding more quickly (hence larger  $\delta_2$ ) as it decelerates in the streamwise direction. This deceleration of the flow also has the effect of reducing  $u_{\tau}$ . As illustrated in Fig. 1b,  $u_{\tau}$  of the significantly decelerated APG case is less than that of the lesser decelerated

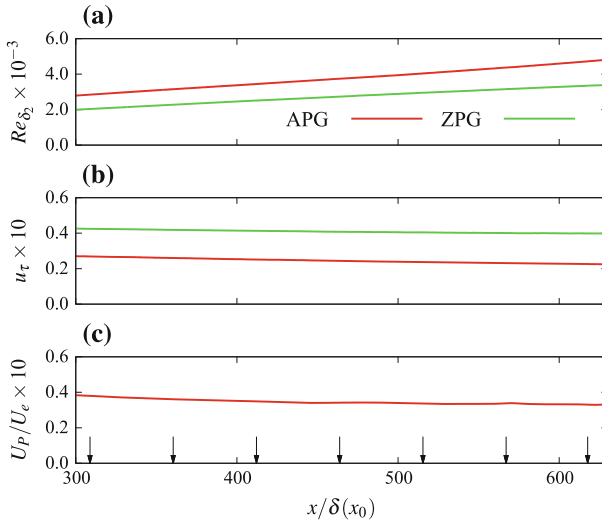


**Fig. 1** Boundary layer properties of the APG DNS (red line) and the ZPG DNS (green line): **a** momentum thickness Reynolds number  $Re_{\delta_2} = U_e \delta_2 / \nu$ ; **b** friction velocity  $u_\tau = \sqrt{\tau_w / \rho}$ ; **c** pressure velocity  $U_p = \sqrt{(\partial P_e / \partial x) \delta_1 / \rho}$  divided by the reference freestream velocity  $U_e$ , with arrows indicating the positions of the APG TBL velocity profiles illustrated in Fig. 2

ZPG TBL. However, the APG TBL DNS has not yet attained the desired  $u_\tau \rightarrow 0$  condition, representative of incipient separation. Further fine tuning of the BC is required. A TBL is deemed self-similar if the ratio of pressure velocity ( $U_p$ ) to  $U_e$  is constant for a boundary layer growing linearly with streamwise position (Mellor and Gibson 1966). The pressure velocity, defined by  $U_p = \sqrt{(\partial P_e / \partial x) \delta_1 / \rho}$ , is a velocity scale based on the reference streamwise pressure gradient  $\partial P_e / \partial x$ . A near constant ratio of  $U_p / U_e$  is achieved over the range  $300\delta(x_0) < x < 650\delta(x_0)$ , see Fig. 1c.

Streamwise velocity variance profiles ( $\langle uu \rangle$ ) are now presented at the streamwise positions indicated by the arrows in Fig. 1c. In Fig. 2a the profiles are non-dimensionalised by  $u_\tau$  and plotted against  $y^+ = y u_\tau / \nu$ . The blue dots in this figure represent results from the previous ZPG DNS of Jiménez et al. (2010), which agree with the present ZPG simulation. When scaled by  $u_\tau$ , the non-dimensional velocity variance profiles from each of the various streamwise stations do not collapse, but in fact increase as  $u_\tau$  decreases in the downstream direction—indicated by the arrow in Fig. 2a. However, the profiles do collapse when scaled by  $U_e$  as illustrated in Fig. 2b, with the black line in this figure illustrating the streamwise average. Note the APG case also exhibits an outer peak not observed in the ZPG results.

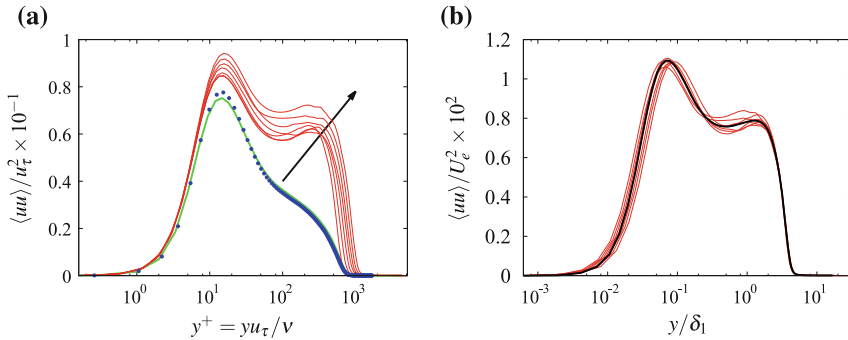


**Fig. 2** Profiles of  $\langle uu \rangle$  under: **a** friction velocity ( $u_\tau$ ) scaling, arrow indicating increasing streamwise position; and **b** outer velocity ( $U_e$ ) scaling. ZPG TBL DNS of Jiménez et al. (2010)—blue dots. ZPG TBL DNS current simulation—green line. APG TBL DNS from current simulation at stream wise locations illustrated in Fig. 1c—red lines. Streamwise averaged scaled profiles—black lines

### 4 Concluding Remarks

An adverse pressure gradient turbulent boundary layer was generated via direct numerical simulation with a modified farfield boundary condition. The boundary layer has a near constant ratio of pressure velocity to freestream velocity, over a momentum thickness based Reynolds number range from 3000 to 5000. Within this domain, streamwise velocity variance profiles were shown to collapse under outer velocity scaling as opposed to friction velocity scaling.

**Acknowledgments** We acknowledge the funding from the Australian Research Council (ARC) and European Research Council, and computational resources provided by the NCI, iVEC and PRACE. Julio Soria gratefully acknowledges the support of an ARC Discovery Outstanding Researcher Award fellowship.

### References

Borrell G, Sillero JA, Jiménez J (2013) A code for direct numerical simulation of turbulent boundary layers at high reynolds numbers in BG/P supercomputers. *Comput Fluids* 80:37–43

Gungor AG, Simens MP, Jiménez J (2012) Direct numerical simulation of wake-perturbed separated boundary layers. *J Turbomach* 134:061024

Jiménez J, Hoyas S, Simens MP, Mizuno Y (2010) Turbulent boundary layers and channels at moderate Reynolds numbers. *J Fluid Mech* 657(22):335–360

Kitsios V, Cordier L, Bonnet J-P, Ooi A, Soria J (2011) On the coherent structures and stability properties of a leading edge separated airfoil with turbulent recirculation. *J Fluid Mech* 683:395–416

Lee J-H, Sung J (2008) Effects of an adverse pressure gradient on a turbulent boundary layer. *Int J Heat Fluid Flow* 29:568–578

- Lele SK (1992) Compact finite difference schemes with spectral-like resolution. *J Comput Phys* 103:16–42
- Mellor GL, Gibson DM (1966) Equilibrium turbulent boundary layers. *J Fluid Mech* 24:225–253
- Sillero J (2014) High Reynolds number turbulent boundary layers. PhD thesis, Universidad Politécnica de Madrid
- Sillero JA, Jiménez J, Moser RD (2013) One-point statistics for turbulent wall-bounded at Reynolds numbers up to  $\delta^+ \approx 2000$ . *Phys Fluids* 25:105102
- Simens MP, Jiménez J, Hoyas S, Mizuno Y (2009) A high-resolution code for tubulent boundary layers. *J Comput Phys* 228:4128–4231